Indian J Phys (June 2015) 89(6):525–538
DOI 10.1007/s12648-014-0618-z

ORIGINAL PAPER

Density functional theory, comparative vibrational spectroscopic studies, highest occupied molecular orbital and lowest unoccupied molecular orbital analysis of Linezolid

K Rajalakshmi[1]*, S Gunasekaran[2] and S Kumaresan[3]

[1]Department of Physics, Sri Chandrasekharendra Saraswathi Viswa MahaVidhyalaya, Kanchipuram 631 561, India

[2]PG and Research Department of Physics, Pachaiyappa's College, Chennai 600 030, India

[3]PG and Research Department of Physics, Arignar Anna Government Arts College, Cheyyar 604 407, India

Received: 06 August 2014 / Accepted: 15 October 2014 / Published online: 9 November 2014

Abstract: The Fourier transform infrared spectra and Fourier transform Raman spectra of Linezolid have been recorded in the regions 4,000–400 and 4,000–100 cm^{-1}, respectively. Utilizing the observed Fourier transform infrared spectra and Fourier transform Raman spectra data, a complete vibrational assignment and analysis of the fundamental modes of the compound have been carried out. The optimum molecular geometry, harmonic vibrational frequencies, infrared intensities and Raman scattering activities, have been calculated by density functional theory with 6-31G(d,p), 6-311G(d,p) and M06-2X/6-31G(d,p) levels. The difference between the observed and scaled wavenumber values of most of the fundamentals is very small. A detailed interpretation of the infrared and Raman spectra of Linezolid is reported. Mulliken's net charges have also been calculated. Ultraviolet–visible spectrum of the title molecule has also been calculated using time-dependent density functional method. Besides, molecular electrostatic potential, highest occupied molecular orbital and lowest unoccupied molecular orbital analysis and several thermodynamic properties have been performed by the density functional theoretical method.

Keywords: FTIR; FT-Raman; DFT; Linezolid; HOMO and LUMO

PACS Nos.: 31.15.E-; 07.57.-c; 34.50.Fa

1. Introduction

In the last decade, quantum mechanical ab initio and density functional theory (DFT) computational methods have gained importance in vibrational spectroscopy and also in the investigations of molecular structure. Vibrational spectroscopy and normal mode calculations for molecules and similar chemical species have become standard features of many quantum chemical program packages. Linezolid [(*S*)-*N*-({3-[3-fluoro-4-(morpholin-4-yl)phenyl]-2-oxo-1,3-oxazolidin-5-yl}methyl)acetamide] is a synthetic antibiotic with the molecular formula $C_{16}H_{20}FN_3O_4$. Linezolid is a member of the oxazolidinone class of drugs, that are resistant to several other antibiotics [1–3]. In the scientific literature, Linezolid has been called a "reserve antibiotic"—that it remains effective as a drug of last resort against potentially intractable infections [4, 5]. To our knowledge, the vibrational spectra and the theoretical calculations of Linezolid have not been reported except in our work. Recently, the DFT methods have evolved to a powerful quantum chemical tool for the determination of the electronic structure of molecules. IR, Raman spectroscopic studies along with highest occupied molecular orbital (HOMO), lowest unoccupied molecular orbital (LUMO) analysis has been used to elucidate information regarding charge transfer within the molecule.

2. Experimental details

The pure sample was obtained from M/s. Sigma Aldrich Co., and was used as such without further purification. The Fourier transform infrared spectrum of the title compound was recorded using (Perkin Elmer) spectrometer in KBr

*Corresponding author, E-mail: k_rajalakshmi123@yahoo.com

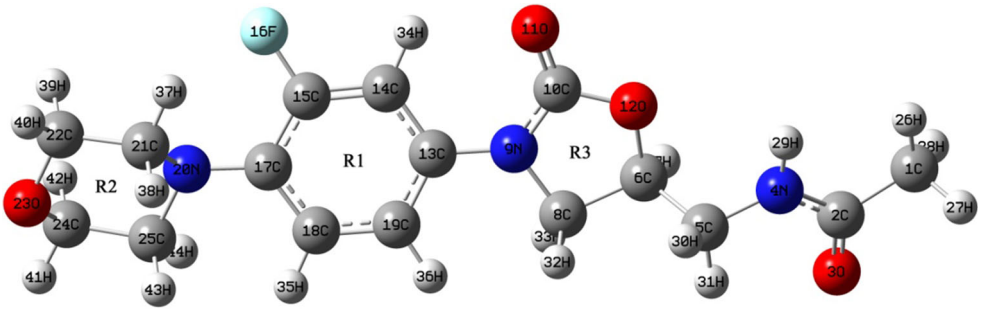

Fig. 1 Geometry of Linezolid optimized at DFT/B3LYP/6-31G(d,p) level

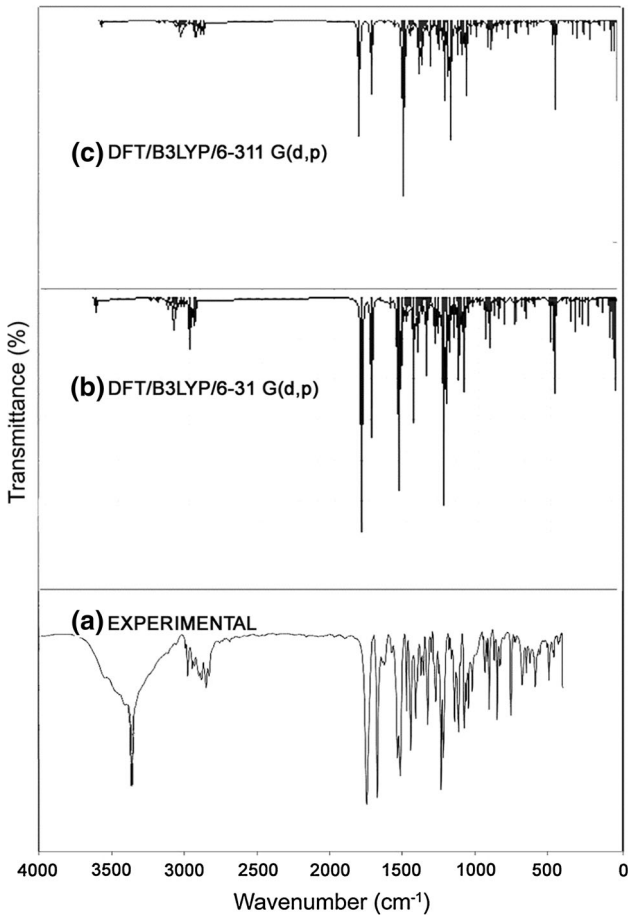

Fig. 2 Comparison of FT-IR spectra of Linezolid (**a**) experimental, (**b**) calculated with B3LYP/6-31G(d,p) and (**c**) calculated with B3LYP/6-311G(d,p) levels

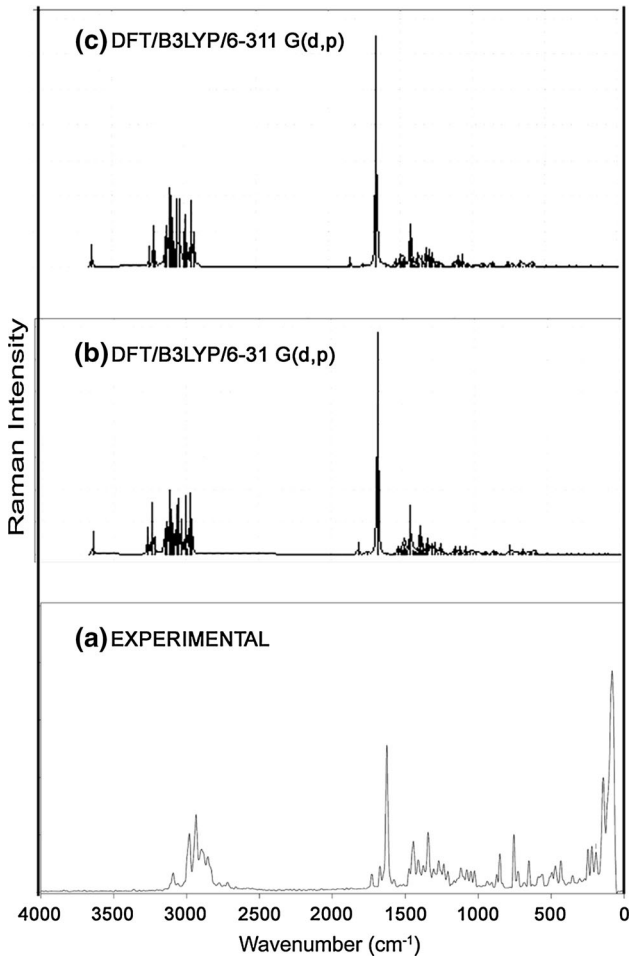

Fig. 3 Comparison of FT-Raman spectra of Linezolid (**a**) experimental, (**b**) calculated with B3LYP/6-31G(d,p) and (**c**) calculated with B3LYP/6-311G(d,p) levels

dispersion in range 4,000–400 cm^{-1}. The FT-Raman spectrum of Linezolid was recorded in 1,054 line of a Nd:YAG laser as excitation wavelength in region 4,000–100 cm^{-1} on a (Bruker model IFS 66V) spectrophotometer equipped with FRA 106 FT-Raman module accessory. The optical properties of the Linezolid were examined using UV–visible spectrophotometer at room temperature. UV–visible spectrum was recorded in the range of 190–800 nm in a (Perkin Elmer-Lambda 950-UV–visible) spectrometer. To measure the UV visible absorption, the Linezolid particles were dispersed in deionized water and measured. The optimized molecular structure of Linezolid has been given in Fig. 1. For visual comparison, the experimental and calculated FTIR of Linezolid at DFT–B3LYP method using 6-31G(d,p) and 6-311G(d,p) levels are shown in Fig. 2(a)–2(c) and the experimental and calculated FT Raman spectra of Linezolid at DFT–B3LYP method using 6-31G(d,p) and 6-311G(d,p) levels are shown in Fig. 3(a)–3(c).

3. Computational details

In the frame work of DFT approach, different exchange and correlation functions were routinely used. Among these, the B3LYP combination [6, 7] was the most used since it proved its ability in reproducing various molecular properties, including vibrational spectra. In order to provide information with regard to the structural characteristics and the normal vibrational modes of Linezolid, the DFT–B3LYP correlation functional calculations were carried out. The experimental molecular geometric data of Linezolid [8] was used for optimization and the entire calculations were performed at ab initio Hartree–Fock (HF) and DFT method using B3LYP/6-31G(d,p), B3LYP/6-311G(d,p) and M06-2X/6-31G(d,p) levels [9–11] on a Pentium V/1.6 GHz personal computer using GAUSSIAN 09W software package [12]. The Raman activities (S_i) calculated with the GAUSSIAN 09W program were subsequently converted to relative Raman intensities (I_i) using the following relationship derived from the basic theory of Raman scattering [13, 14],

$$I_i = \frac{f(v_0 - v_i)^4 S_i}{v_i[1 - \exp(-hcv_i/kT)]}$$

where v_0 denoting exciting frequency in cm^{-1}, v_i denoting vibrational wave number of ith normal mode in cm^{-1}, h, c, k and T being Planck and Boltzmann constants, speed of light and temperature in Kelvin and f takes a constant equal to 10^{-12} and chosen as common normalization factor for all peak intensities.

4. Results and discussion

The optimized geometrical parameters have been calculated at B3LYP with 6-31G(d,p) and B3LYP with 6-311G(d,p) levels. The calculated geometric parameters (bond lengths and bond angles) for Linezolid are listed in Table 1. The calculated values have been compared with X-ray diffraction results [15]. From the structural data, it is found that most of the optimized bond lengths are larger than the experimental values. This is due to the fact that the theoretical calculations result from isolated molecules in gaseous phase, while the experimental results are from molecule in solid state. Comparing bond lengths and bond angles of B3LYP/6-31G(d,p) and 6-311G(d,p) levels for Linezolid, it is also observed that the geometrical parameters are found to be almost same at B3LYP/6-31G(d,p) and B3LYP/6-311G(d,p) levels. However, the B3LYP/6-31G(d,p) level of theory, in general slightly over estimates bond lengths but it yields bond angles in excellent agreement with the B3LYP/6-311G(d,p) level.

Table 1 Optimized geometrical parameters of, bond length (Å) and bond angle (°) of Linezolid

Optimized parameters	Method/basis sets		
	DFT/B3LYP/6-31G(d,p)	DFT/B3LYP/6-311G(d,p)	Experimental
Bond length (Å)			
R(1,2)	1.5172	1.5179	1.5070
R(1,26)	1.0920	1.0916	1.0899
R(1,27)	1.0935	1.0918	1.0899
R(1,28)	1.0934	1.0916	1.0900
R(2,3)	1.2325	1.2187	1.2128
R(2,4)	1.3633	1.3708	1.3476
R(4,5)	1.4492	1.4479	1.4650
R(4,29)	1.0094	1.0077	0.9700
R(5,6)	1.5234	1.521	1.5300
R(5,30)	1.0958	1.0957	1.0900
R(5,31)	1.0926	1.0921	1.0899
R(6,7)	1.0942	1.0935	1.0899
R(6,8)	1.5371	1.5354	1.5408
R(6,12)	1.4511	1.4442	1.4569
R(8,9)	1.4619	1.4568	1.4709
R(8,32)	1.0975	1.0979	1.0900
R(8,33)	1.0921	1.0918	1.0900
R(9,10)	1.3779	1.3856	1.3399
R(9,13)	1.414	1.4144	1.4019
R(10,11)	1.2156	1.1999	1.2151
R(10,12)	1.3619	1.3681	1.3379
R(13,14)	1.4056	1.4033	1.3883
R(13,19)	1.4003	1.3974	1.3883
R(14,15)	1.3814	1.3777	1.3824
R(14,34)	1.08	1.0788	1.0800
R(15,16)	1.3594	1.3565	1.3510
R(15,17)	1.4075	1.4059	1.3905
R(17,18)	1.4029	1.3996	1.3879
R(17,20)	1.4116	1.4078	1.4008
R(18,19)	1.3961	1.3938	1.3811
R(18,35)	1.0831	1.0816	1.0800
R(19,36)	1.0829	1.0815	1.0800
R(20,21)	1.4756	1.4734	1.4710
R(20,25)	1.4645	1.461	1.4701
R(21,22)	1.5245	1.5237	1.5309
R(21,37)	1.09	1.0883	1.0900
R(21,38)	1.1033	1.1027	1.0899
R(22,23)	1.4258	1.4228	1.4300
R(22,39)	1.1014	1.0999	1.0900
R(22,40)	1.0934	1.0913	1.0900
R(23,24)	1.4248	1.4196	1.4302
R(24,25)	1.5269	1.5271	1.5310
R(24,41)	1.0933	1.0916	1.0899
R(24,42)	1.1013	1.1002	1.0900

Table 1 continued

Optimized parameters	Method/basis sets		
	DFT/B3LYP/6-31G(d,p)	DFT/B3LYP/6-311G(d,p)	Experimental
R(25,43)	1.1041	1.1040	1.0900
R(25,44)	1.0942	1.0931	1.0899
Bond angle (°)			
A(2,1,26)	113.6514	113.8865	109.4724
A(2,1,27)	108.7707	108.4996	109.4727
A(2,1,28)	108.7489	108.5534	109.4730
A(26,1,27)	109.0064	109.1143	109.4714
A(26,1,28)	109.0188	109.1882	109.4711
A(27,1,28)	107.4652	107.4012	109.4665
A(1,2,3)	121.8138	122.0896	119.9994
A(1,2,4)	115.5825	115.3406	119.9979
A(3,2,4)	122.6022	122.5677	120.0026
A(2,4,5)	122.8303	122.1744	119.9975
A(2,4,29)	119.2029	119.8394	120.0074
A(5,4,29)	117.9275	117.7371	119.9950
A(4,5,6)	112.6896	112.1580	109.4700
A(4,5,30)	110.0815	110.3447	109.4716
A(4,5,31)	107.2387	106.7805	109.4742
A(6,5,30)	109.0915	108.9278	109.4651
A(6,5,31)	109.0715	109.9002	109.4750
A(30,5,31)	108.5725	108.6603	109.4711
A(5,6,7)	110.1601	109.9494	110.4623
A(5,6,8)	114.1183	114.5902	110.5187
A(5,6,12)	109.3186	108.9357	110.5256
A(7,6,8)	111.4685	111.283	110.5179
A(7,6,12)	107.0851	107.274	110.6448
A(8,6,12)	104.2867	104.4017	104.0093
A(6,8,9)	101.9939	102.012	103.7780
A(6,8,32)	111.9671	111.8896	110.5699
A(6,8,33)	111.8488	111.7253	110.5656
A(9,8,32)	110.9102	111.1179	110.5671
A(9,8,33)	111.3865	111.5689	110.5607
A(32,8,33)	108.6615	108.4771	110.61525
A(8,9,10)	111.0604	111.2077	108.88526
A(8,9,13)	122.3182	122.3068	125.5537
A(10,9,13)	125.9701	125.7418	125.5604
A(9,10,11)	128.8666	128.9615	123.0772
A(9,10,12)	109.3337	108.6467	113.8487
A(11,10,12)	121.7998	122.3918	123.0737
A(6,12,10)	110.5333	110.7039	109.4765
A(9,13,14)	121.7262	121.7388	119.9857
A(9,13,19)	119.835	119.9189	119.9973
A(14,13,19)	118.4207	118.3292	120.016
A(13,14,15)	119.2298	119.3576	119.9842
A(13,14,34)	121.4043	121.3907	120.0110
A(15,14,34)	119.3612	119.2486	120.0046

Table 1 continued

Optimized parameters	Method/basis sets		
	DFT/B3LYP/6-31G(d,p)	DFT/B3LYP/6-311G(d,p)	Experimental
A(14,15,16)	117.1419	117.1905	120.0220
A(14,15,17)	124.227	124.1456	119.9571
A(16,15,17)	118.6287	118.6608	120.0208
A(15,17,18)	115.1247	115.1356	119.9773
A(15,17,20)	120.5874	120.7736	120.0114
A(18,17,20)	124.2181	124.0397	120.0105
A(17,18,19)	122.2383	122.2463	120.0185
A(17,18,35)	119.6335	119.4857	119.9916
A(19,18,35)	118.1275	118.2676	119.9892
A(13,19,18)	120.7402	120.7688	120.0434
A(13,19,36)	120.8677	120.8808	119.9714
A(18,19,36)	118.386	118.3437	119.9844
A(17,20,21)	116.27	116.9183	110.9894
A(17,20,25)	116.8126	117.3662	110.9963
A(21,20,25)	110.8979	111.32	110.7760
A(20,21,22)	109.6355	109.5796	109.2090
A(20,21,37)	109.599	109.6165	109.5592
A(20,21,38)	110.5342	110.3467	109.4959
A(22,21,37)	109.4275	109.5392	109.5082
A(22,21,38)	109.3495	109.3187	109.5115
A(37,21,38)	108.2704	108.4198	109.5428
A(21,22,23)	111.4453	111.4344	109.2928
A(21,22,39)	109.5503	109.4084	109.5088
A(21,22,40)	110.2481	110.4797	109.5040
A(23,22,39)	110.0109	110.0157	109.5094
A(23,22,40)	106.7856	106.5095	109.5063
A(39,22,40)	108.733	108.9321	109.5056
A(22,23,24)	110.434	110.6408	113.7406
A(23,24,25)	111.5645	111.5694	109.2552
A(23,24,41)	106.8072	106.5935	109.5078
A(23,24,42)	110.0678	110.0979	109.5044
A(25,24,41)	110.1317	110.331	109.5081
A(25,24,42)	109.4891	109.3105	109.5397
A(41,24,42)	108.7119	108.8784	109.5115
A(20,25,24)	109.4273	109.3986	109.2562
A(20,25,43)	111.9207	111.9513	109.5054
A(20,25,44)	109.3469	109.2014	109.5117
A(24,25,43)	108.9715	108.8442	109.5067
A(24,25,44)	109.1087	109.1931	109.5048
A(43,25,44)	108.0169	108.2082	109.5419

As can be seen in Table 1, it is observed that the C–C bond distances in the molecule varies in the narrow range 1.377–1.534 Å calculated by B3LYP/6-311G(d,p) method. The C–C bond length in the ring R1 ranges from 1.377 to

1.405 Å. The C5–C6 bond length is 1.521 Å. This is smaller than the C–C bond distances of R3 ring. This clearly shows that there is a delocalization of the p-electrons of N–C towards the ring of R3. The inter nuclear distance determined by B3LYP/6-311G(d,p) method between O11 and H34, N9 and H36 in the optimized geometries are 2.207 and 2.674 Å, respectively. This longer distance is not in favor for the formation of intra molecular hydrogen bond of the type N–H and O–H. The calculated bond angle of ring R1 by B3LYP/6-311G(d,p) method lie in the range 118.34°–124.14°. The bond angle of C10–N9–C3, N9–C10–O11 and C14–C15–C17 are the highest, where the nitrogen Oxygen atom and Flourine atom are attached and are equal to 125.741, 128.961 and 124.145, respectively. This variation in bond angle depends on the electro negativity of the atom. If the electro negativity of the atom increases, bond angle increases.

4.1. Vibrational assignments

The molecule Linezolid has 44 atoms with 126 normal modes of vibration. According to group theory the point group symmetry for the molecule is C1 and all 126 fundamental modes of vibrations are active both in the Infrared absorption and Raman scattering. The detailed vibrational assignments of fundamental modes of Linezolid along with calculated IR and Raman frequencies and normal mode are reported in Table 2.

The main focus of the present investigation is the proper assignment of the experimental frequencies to the various vibrational modes of the title molecule at DFT/B3LYP/6-31G(d,p) level and DFT/B3LYP/6-311G(d,p) level. Comparison of the frequencies calculated by DFT–B3LYP method with the experimental values reveals the overestimation of the calculated vibrational modes due to neglect of anharmonicity in real system. Normally, the over estimation of unscaled frequencies when, compared to observed frequencies, were prominent only in the higher frequency region [16]. The results indicate that the B3LYP/6-311G(d, p) calculations approximate the observed fundamental frequencies much better than the B3LYP/6-31G(d, p) results. Therefore, it is customary to scale down the calculated harmonic wavenumber in order to improve the agreement with the experimental values. The harmonic vibrational frequencies have been scaled by 0.9712 and 0.9738 for B3LYP/6-31G(d,p) B3LYP/6-311G(d,p) and 0.9701 for M06-2X/6-31G(d,p) levels [17].

4.1.1. N–H vibrations

In mono fluorinated amines the stretch frequency of NH may vary and it not so intense. When the hydroxyl bonds on the same region are less intense the amines have low intense peaks due to halogens presence. According to Socrates [18], the stretching of amino group appears around 3,500–3,000 cm^{-1}. The position of absorption in this region depends upon the degree of the hydrogen bonding, and hence upon the physical state of the sample or the polarity of the solvent. In the present study, the N–H stretching frequency has been observed at 3,542 and 3,543 cm^{-1} from DFT/B3LYP/6-31G(d, p) level and M06-2X level. The corresponding band in FT-IR spectrum is observed at 3,543 cm^{-1}. Computational data for N–H in plane bending is assigned at 1,404 cm^{-1} by B3LYP/6-31G(d,p) level and experimentally it is assigned at 1,444 cm^{-1} in FT-IR and 1,444 cm^{-1} in FT Raman respectively. Theoretical data for N–H out of plane bending are presented in Table 2 and are found to agree well within the characteristic region [19].

4.1.2. Carbon–hydrogen vibrations

The heteroaromatic organic compounds and its derivatives are structurally very close to benzene and commonly exhibit multiple weak bands in the region 3,100–3,000 cm^{-1} due to C–H stretching vibrations [20]. In our study, the vibrational frequencies found at 3,173, 3,140, 3,128 and 3,060 cm^{-1} are assigned to C–H stretching vibrations of the molecule by B3LYP/6-31G(d,p) and B3LYP/6-311G(d,p) levels. The vibrational frequencies found at 3,146, 3,114, 3,100 and 3,067 cm^{-1} are assigned to C–H stretching vibrations of the molecule by M06-2X/6-31G(d,p) level. In FT-IR, frequency vibrations occurring at 3,180, 3,155 and 2,852 cm^{-1} are assigned to C–H vibrations and it shows good agreement with the literature data. The C–H in-plane and out-of-plane bending vibrations generally lie in the range 1,300–1,000 and 1,000–750 cm^{-1} [21, 22], respectively. The FTIR bands at 1,273, 1,220, 1,143, 1,078 and 1,022 cm^{-1} and FT-Raman bands at 1,207, 1,118, 1,077, 1,049 and 1,024 cm^{-1} are assigned to C–H in-plane bending vibrations of the molecule. The theoretically computed values by B3LYP/6-31G(d,p) and B3LYP/6-311G(d,p) levels are 1,245, 1,239, 1,216, 1,201, 1,046, 1,025 and 1,007 cm^{-1}, which is in good agreement with literature values. The peaks at 935, 906, 756 in FTIR and 937,871 and 754 cm^{-1} in FT-Raman confirm the C–H out of plane bending vibrations, which agrees with the above said literature values. In general, the C–H vibrations (stretching, in plane and out-of-plane bending vibrations) calculated theoretically are in good agreement with experimental values.

4.1.3. Carbonyl group vibration

The characteristic infrared absorption frequencies of carbonyl group has been investigated earlier and the C=O stretching vibration are expected in the region 1,750–1,680 cm^{-1} [23, 24]. In Linezolid, the C=O stretching vibration is calculated at 1,690 cm^{-1} in B3LYP/

Table 2 Vibrational assignments of fundamental modes of Linezolid along with calculated IR, Raman intensities at DFT/B3LYP with 6-31G(d,p), 6-311G(d,p) and IR intensities at MO6-2X/6-31G(d,p) levels

Sl. no.	Observed fundamentals (cm^{-1})		Calculated frequencies (cm^{-1})								Vibrational assignments
			B3LYP/6-31G(d,p)			B3LYP/6-311G(d,p)			MO6-2X/6-31G(d,p)		
	FTIR	Raman	Scaled	IR intensity	Raman activity	Scaled	IR intensity	Raman activity	Scaled	IR intensity	
1	3,543		3,542	60.666	121.747	3,542	31.660	52.133	3,543	33	υ (NH)
2	3,410		3,173	13.512	147.326	3,159	16.265	49.616	3,146	17	υ (CH)
3	3,363		3,140	7.276	274.986	3,125	5.318	100.175	3,114	6	υ (CH)
4			3,128	14.083	94.945	3,111	14.342	36.164	3,100	13	υ (CH)
5		3,091	3,060	14.345	118.394	3,048	7.239	44.166	3,067	6	υ (CH)
6	2,978		3,059	23.882	104.817	3,038	16.921	64.028	3,046	8	υasy ($C_1H_{26,27}$)
7			3,047	8.716	148.513	3,035	6.331	93.904	3,042	7	υasy ($C_1H_{26,27}$)
8			3,044	5.694	99.706	3,022	5. 404	43.409	3,023	3	υasy($C_5H_{30,31}$)
9			3,028	24.895	143.914	3,013	37.756	190.082	3,006	36	υasy($C_8H_{32,33}$)
10			3,021	56.830	339.721	3,009	43.773	173.036	3,001	40	υasym($C_{22}H_{39,40}$) υasym($C_{24}H_{41,42}$)
11			3,019	58.371	239.474	2,998	26.531	62.488	2,998	22	υasym($C_{22}H_{39,40}$) υasym($C_{24}H_{41,42}$)
12			3,005	36.614	134.795	2,989	23.046	54.523	2,983	22	υasym($C_{22}H_{39,40}$) υasym($C_{24}H_{41,42}$)
13		2,980	2,996	46.730	93.287	3,974	30.027	29.511	2,974	14	υsym($C_5H_{30,31}$)
14			2,975	5.941	258.250	2,965	7.346	165.820	2,960	4	υsym($C_1H_{26,27,28}$)
15		2,934	2,969	28.604	298.250	2,945	25.821	162.890	2,946	24	υsym($C_5H_{30,31}$)
16			2,949	39.023	189.506	2,916	31.991	85.016	2,924	26	υsym($C_8H_{32,33}$)
17		2,897	2,914	176.197	308.532	2,906	100.746	127.811	2,889	93	υsym($C_{22}H_{39,40}$) υsym($C_{24}H_{41,42}$)
18			2,910	25.507	29.965	2,899	29.169	39.576	2,884	30	υsym($C_{22}H_{39,40}$) υsym($C_{24}H_{41,42}$)
19	2,852	2,853	2,894	117.643	327.573	2,869	72.021	159.729	2,863	57	υsym($C_{22}H_{39,40}$) υsym($C_{24}H_{41,42}$)
20	2,831	2,719	2,876	81.356	190.045	2,852	49.736	85.569	2,841	49	υsym($C_{22}H_{39,40}$) υsym($C_{24}H_{41,42}$)
21	1,747	1,729	1,756	794.884	64.122	1,797	446.860	23.573	1,858	426	β(C–N) υ(C=O) β(C–O)
22	1,676	1,673	1,690	448.027	12.903	1,716	269.828	6.087	1,775	225	υ(C=O) β(C–N) β(C–C) γ(N–H)
23	1,620	1,625	1,627	10.691	1,167.821	1,622	10.333	559.641	1,650	12	δ(R1)
24			1,567	31.202	9.359	1,560	19.971	3.004	1,594	28	δ_{asy}(R1) γ(C–H) γ(C–N)
25	1,516		1,512	239.100	4.634	1,505	34.145	3.938	1,521	457	γ(NH) υ(C–N) β(C–H)
26	1,444	1,444	1,448	25.456	21.321	1,447	10.160	2.391	1,421	11	ξ(CH_2) β(C–H)
27			1,447	2.079	51.496	1,444	3.177	18.122	1,415	1	ξ(CH_2) β(N–H)
28			1,438	22.097	21.832	1,436	14.228	13.580	1,412	0	ξ(CH_2) β(C–H)
29			1,434	9.131	27.602	1,432	13.680	11.331	1,404	19	ξ(CH_2) β(C–H)
30			1,429	24.716	18.844	1,432	10.037	6.990	1,399	271	ω(CH_2) β(C–H) β(N–H)
31			1,404	334.137	262.745	1,393	161.044	104.103	1,385	7	ξ(CH_2)
32			1,386	45.555	22.346	1,382	29.996	20.219	1,367	8	ξ(CH_2) β(N–H)
33			1,376	141.597	12.455	1,373	129.208	2.435	1,357	171	ξ(CH_2) β(C–H)
34	1,409	1,410	1,366	20.367	14.610	1,363	21.641	3.786	1,349	21	ξ(CH_2) β(C–H)
35			1,362	26.456	4.091	1,354	14.215	0.976	1,343	42	ω(CH_2) β(C–H)
36			1,347	41.705	27.368	1,342	23.586	13.341	1,339	3	β(C–H)
37	1,376	1,367	1,339	3.063	136.912	1,338	1.826	35.120	1,332	9	ω(CH_2)

Table 2 continued

Sl. no.	Observed fundamentals (cm^{-1})		Calculated frequencies (cm^{-1})								Vibrational assignments
			B3LYP/6-31G(d,p)			B3LYP/6-311G(d,p)			MO6-2X/6-31G(d,p)		
	FTIR	Raman	Scaled	IR intensity	Raman activity	Scaled	IR intensity	Raman activity	Scaled	IR intensity	
38			1,332	5.281	23.761	1,331	2.136	6.999	1,322	8	ω(CH_2)
39			1,323	196.116	58. 576	1,318	131.098	27.819	1,303	1	ω(CH_2)
40		1,343	1,307	21.346	5.536	1,299	3.070	1.229	1,294	32	δ_{asy}(R1) γ(C–N)δ(R_3) γ(C–H)
41			1,296	27.030	29.622	1,296	16.674	9.215	1,283	16	ρ(CH_2) β(C–H)
42	1,328		1,289	11.209	75.867	1,284	11.556	41.232	1,282	25	ω(CH_2) β(C–H) β(C–N)
43			1,264	105.872	61.117	1,266	52.529	35.695	1,260	70	τ(CH_2)υ(C–N) β(C–F) γ(C–H)
44			1,262	76.597	24.505	1,260	77.733	8.976	1,251	55	τ(CH_2)υ(C–N) β(C–H)
45	1,273	1,270	1,245	47.911	66.719	1,243	25.878	32.770	1,233	86	τ(CH_2) β(C–N) β(C–H)
46			1,239	84.480	16.596	1,224	41.596	10.245	1,230	75	γ(N–H) β(C=O) β(C–H) β(N–H)
47			1,216	119.332	8.244	1,221	211.145	1.963	1,222	82	ρ(CH_2) υ(C–N) υ(C–F) β(C–H)
48	1,236	1,235	1,204	86.564	37.802	1,203	4.409	12.862	1,216	75	ρ(CH_2) υ(C–N) υ(C–F) β(C–H)
49	1,220		1,201	475.151	14.865	1,195	71.006	5.974	1,196	295	ρ(CH_2) υ(C–N) υ(C–F) β(C–H)
50			1,198	30.318	20.783	1,192	142.521	6.030	1,190	36	τ(CH_2) β(N–H)
51		1,207	1,185	237.722	6.438	1,180	303.881	2.813	1,179	27	τ(CH_2) β(C–H) β(N–H) υ(C–F)
52			1,165	122.262	1.670	1,163	73.270	0.850	1,178	73	β(C–O) β(C–N) β(C–H) υ(C–F)
53			1,135	84.336	2.787	1,132	84.735	1.096	1,156	96	β(C–O) β(C–N) β(C–H) υ(C–F)
54	1,143		1,112	6.565	6.266	1,114	6.189	1.316	1,132	41	β(C–H) υ(C–F) γ(N–H)
55			1,106	16.852	9.461	1,106	22.627	3.934	1,118	17	ρ(CH_3) ρ(CH_2) β(C–H) γ(N–H)
56			1,104	174.255	1.882	1,104	82.667	1.123	1,105	163	υ(C–O–C) β(C–H)
57	1,122		1,100	118.968	37.746	1,098	65.826	10.247	1,102	16	ρ(CH_2) υ(C–O)
58		1,118	1,086	44.108	9.677	1,089	39.388	3.525	1,097	50	ρ(CH_2) β(N–H)
59			1,069	190.296	45.953	1,072	172.631	27.925	1,082	19	υ(C–O) β(C=O) γ(C–H)
60			1,064	17.030	4.786	1,062	7.701	2.165	1,056	4	ρ(CH_2) υ(C–C) β(C–H)
61	1,078	1,077	1,046	21.662	2.685	1,045	4.181	0.895	1,042	13	ρ(CH_2) υ(C–C) β(C–H)
62			1,037	28.920	45.683	1,038	32.491	29.881	1,023	14	δ(R_2) ρ(CH_2)
63		1,049	1,025	12.204	0.634	1,026	6.688	0.159	1,017	3	τ(CH_2) β(C–H)
64			1,008	10.700	8.499	1,007	3.312	8.989	1,013	9	δ(R_1 R_2 R_3)
65	1,022	1,024	1,007	15.549	22.020	1,001	34.701	4.603	1,010	6	δ(R_2) ω(CH_2) β(C–O) β(C–H)
66			982	6.973	38.322	976	14.522	2.082	970	11	ω(CH_2) β(C=O) γ(C–H)
67			961	14.519	8.122	959	7.834	3.721	950	12	τ(CH_2) γ(C–H) ω(CH_2) γ(N–H)
68			923	71.208	7.920	926	54.199	2.935	942	75	δ(R_3) β(C–N) γ(C–H) β(C–O) γ(C–H)
69	935	937	912	11.825	1.644	914	9.956	0.279	917	11	δ(R_3) β(C–N) γ(C–H) β(C–O) γ(C–H)
70			904	43.911	6.898	902	57.811	5.184	895	17	δ(R_3) β(C–N) γ(C–H) β(C–O) γ(C–H)

Table 2 continued

Sl. no.	Observed fundamentals (cm^{-1})		Calculated frequencies (cm^{-1})								Vibrational assignments
			B3LYP/6-31G(d,p)			B3LYP/6-311G(d,p)			MO6-2X/6-31G(d,p)		
	FTIR	Raman	Scaled	IR intensity	Raman activity	Scaled	IR intensity	Raman activity	Scaled	IR intensity	
71	906		893	84.354	9.524	894	39.911	4.429	883	5	$\tau(CH_2)$ υ(C–O) γ(N–H)
72	850	850	866	29.232	8.619	868	22.228	4.352	867	2	RING BREATHING(R_3)
73		871	845	0.214	8.790	863	19.092	1.744	859	12	$\delta(R_3)$ $\tau(CH_2)$ γ(C–H)
74			842	11.886	11.417	843	2.123	6.971	849	20	υ(C–O) $\delta(R_2)$ γ(C–H)
75			838	33.992	13.896	839	4.456	8.763	841	5	RING BREATHING(R_2)
76			826	15.538	6.490	828	16.542	2.269	839	1	$\delta(R_1\ R_3)$ γ(C–H) γ(N–H)
77	756	754	792	40.849	3.973	787	29.952	0.631	777	24	$\delta(R_1\ R_3)$ γ(C–H)
78		726	732	36.670	47.438	736	17.232	11.234	753	32	$\delta(R_1\ R_2\ R_3)$ $\tau(CH_2)$ β(C–N)
79			716	9.996	9.534	732	19.639	10.120	732	18	β(C–N) β(C=O) β(C–O)
80			714	32.079	1.798	716	3.116	4.841	726	3	β(C–N) β(C=O) β(C–O)
81	678	683	680	11.087	10.625	700	9.673	5.106	696	4	$\delta(R_1\ R_2\ R_3)$ β(C–H)
82	650	651	663	16.507	5.334	662	8.373	2.582	678	6	$\delta(R_3)$ β(C=O) β(C–O) β(C–N) γ(C–H)
83	588	560	573	1.828	8.338	574	1.074	4.685	574	1	$\delta(R_3)$ $\tau(CH_2)$
84			560	1.178	15.610	563	0.529	8.902	559	0	$\delta(R_1\ R_2\ R_3)$ β(C=O) β(C–F) β(C–H)
85	493		491	6.239	3.736	492	4.164	1.730	502	23	$\delta(R_1\ R_2\ R_3)$ β(C=O) β(C–F) β(C–H)
86			486	41.436	3.149	488	25.409	1.173	488	13	$\delta(R_1\ R_2\ R_3)$ β(C=O) β(C–F) β(C–H)
87		469	478	4.917	4.241	479	6.387	2.250	478	2	β(N–H) γ(C=O) γ(C–H)
88			461	46.352	3.398	466	88.966	1.879	465	94	$\delta(R_3)$ γ(C–H)
89			458	83.923	2.322	463	7.417	0.198	460	1	β(N–H) γ(C–H)
90		432	443	18.027	0.496	447	0.970	0.507	446	10	β(N–H) β(C=O) β(C–H)
91			411	1.953	4.998	409	1.573	2.823	419	1	β(N–H) β(C=O) β(C–H)
92			401	0.787	2.684	400	0.592	0.962	406	0	β(N–H) β(C=O) β(C–H)
93			382	4.355	1.262	381	2.346	0.693	381	5	$\tau(CH_2)$ β(C–N) β(C–O)
94		352	349	15.475	3.926	349	10.197	1.644	345	4	$\tau(CH_2)$ β(C–N) β(C–O)
95			268	2.474	1.003	264	0.563	0.251	272	3	β ($R_1\ R_2\ R_3$)
96		246	248	2.399	3.562	247	1.135	1.283	265	2	β ($R_1\ R_2\ R_3$)

6-31G(d,p) level and 1,775 cm^{-1} at M06-2X/6-31G(d,p) level. A strong band in IR spectrum at 1,747 cm^{-1} and a band in FT-Raman spectrum at 1,729 cm^{-1} is assigned to C=O stretching vibration. The carbon–oxygen bond is formed by pπ–pπ* between carbon and oxygen and the lone pair of electron on oxygen also determines the nature of carbonyl group. The higher degree of conjugation is due to the maximum overlap of p-orbital, occurring because of the planarity of the group (–CH=C=(C=O)–C=CH–). The conjugation increases the single bond character of C=O bond [25] and consequently lowers the wave number of the carbonyl absorption. The calculated values always overestimate the observed values due to anharmonicity in the real system.

4.1.4. Carbon–nitrogen vibrations

The identification of C–N vibrations is a very difficult task, since mixing of several bands are possible in this region. Silverstein et al. [26] assigned C–N stretching absorption in the region 1,382–1,266 cm^{-1} for aromatic amines. In this study, the bands observed at 1,323 and 1,204 cm^{-1} in B3LYP/6-31G(d,p) are assigned for C–N stretching. A band observed at 1,236 cm^{-1} IR and at 1,235 cm^{-1} at FT-

Raman has been assigned to C–N stretching vibration of Linezolid. The slight shift in wavenumber is due to the fact that force constants of the C–N bond increases due to resonance with the ring. Pyrimidine absorb strongly in the region 1,600–1,500 cm^{-1} due to the C=C and C=N ring stretching vibrations [27]. The C–N in-plane and out-of-plane bending vibrations have also been identified and are listed in Table 2.

4.1.5. Ring vibrations

The ring stretching vibrations *v* (Ring) are complicated combinations of stretching of C–N, C=C, C–O and C–C bonds. Many ring modes are affected by the substitution in the aromatic ring. In the present study, the rings are named as R1 (six_membered ring), R2 (Morpholin ring) R3 (oxazolidinone ring). The bands absorbed at 1,627, 1,567, 1,506, 1,339, 923 cm^{-1} in R1 and 1,465, 1,456, 1,488, 1,392, 1,376, 1,362, 1,332, 1,296, 1,104, 923 cm^{-1} for R2 and 1,386, 1,201, 961 cm^{-1} in R3 have been designated to ring stretching and bending modes respectively. The most important ring stretching vibration is the ring breathing vibration, where all bonds of the rings appear to stretch and contract in-phase with each other [30]. In the experimental infrared spectrum of Linezolid, this mode appears at 850 cm^{-1} both in FTIR and FT-Raman spectrum. The ring breathing vibrations are observed at 1,339 cm^{-1} in R1, 838 cm^{-1} in R2 and 866 cm^{-1} (mode 78) in R3 respectively [28].

4.1.6. C–X (F) vibrations

Vibrations belong to C–X (F, Br) bonds, which are formed between the ring and the halogen atoms are interesting since mixing of vibrations are possible due to the lowering of the molecules symmetry and the presence of heavy atoms. The assignments of C–F vibrations have been made by comparison with halogen substituted benzene derivatives. C–F stretching vibrations appear in the lower range of frequencies i.e. 1,000–1,400 and 760–505 cm^{-1} and C–F deformation occur in the range of 700–500 and 300–140 cm^{-1} respectively. The bands of observed spectra identified the stretching and bending vibrations arising at 1,220, 1,143, 493 cm^{-1} in FTIR and 1,207 cm^{-1} in FT-Raman. The calculated values for stretching and bending vibrations by B3LYP/6-31G(d,p) are found at 1,201, 1,135 cm^{-1} and 560, 491 cm^{-1} respectively for Linezolid [29].

4.1.7. CH_2 group vibrations

The title molecule consists of rings R1, R2 and R3. For the assignments of CH_2 group frequencies, basically six fundamentals can be associated to each CH_2 group, namely, CH_2 symmetrical stretching, CH_2 asymmetrical stretching, CH_2 scissoring stretching, CH_2 rocking vibrations, which belong to in-plane vibrations. In addition to that CH_2 wagging modes and CH_2 twisting modes of CH_2 group would be expected to be depolarized for out-of-plane bending vibrations. The asymmetric CH_2 stretching vibration of CH_2 are observed at 3,059, 3,047, 3,044, 3,028 and 3,021 cm^{-1} in all the rings and the symmetric CH_2 stretching vibration of CH_2 are observed at 2,975, 2,969, 2,949, 2,914, 2,910, 2,894, 2,876 cm^{-1} in all rings. The observed band at 2,978 cm^{-1} in IR spectrum is assigned to asymmetric CH_2 stretching vibration. The observed band at 2,852, 2,831 cm^{-1} in IR spectrum and the bands observed at 2,980, 2,934, 2,897, 2,853 cm^{-1} in FT-Raman are assigned to symmetric CH_2 stretching vibration. The CH_2 wagging is observed at 1,339 cm^{-1} in DFT/B3LYP/6-31G level and it is observed a band at 1,376 cm^{-1} in FT-IR spectrum and in Raman spectrum, it is observed a band at 1,367 cm^{-1} that is assigned to CH_2 wagging. The band assigned for CH_2 scissoring are observed at 1,444 cm^{-1} in both FT-IR and Raman spectrum and the calculated band for CH_2 scissoring is 1,404 cm^{-1}. The CH_2 rocking vibrations are observed at 1,204 cm^{-1} from DFT/B3LYP/6-31G level and 1,236 cm^{-1} in FT-IR spectrum and 1,235 cm^{-1} in Raman spectrum. The twisting mode of CH_2 vibrations is observed at 1,245 cm^{-1} from DFT/B3LYP/6-31G level and from FT-IR spectrum it is found to be 1,273 cm^{-1}. In Raman spectrum the twisting mode of CH_2 vibrations is observed at 1,270 cm^{-1} [30].

5. Other molecular properties

5.1. Electrostatic potential, total electron density and molecular electrostatic potential

In the present study, the electrostatic potential (ESP), electron density (ED) and the molecular electrostatic potential (MEP) map figures for Linezolid calculated at DFT/B3LYP/6-311G(d,p) level are shown in Fig. 4(a)–4(c) respectively. It can be seen from the ESP figures, that while the negative ESP is localized more over the oxygen atoms and is reflected as a yellowish blob, the positive ESP is localized on the rest of the molecules. Molecular electrostatic potential (MEP) is related to the electronic density and is very useful descriptor in understanding sites for electrophilic attack and nucleophilic reactions as well as hydrogen bonding interactions [31, 32]. The negative (red)1 regions of MEP are related to electrophilic reactivity and the positive (blue) ones to nucleophilic reactivity, as shown in Fig. 4. As seen from the figure, the negative region is mainly localized on oxygen atoms (O3, O11, O12 and O23) whereas nucleophilic reactivity of the molecule is mainly localized on proton of C=O–NH group.

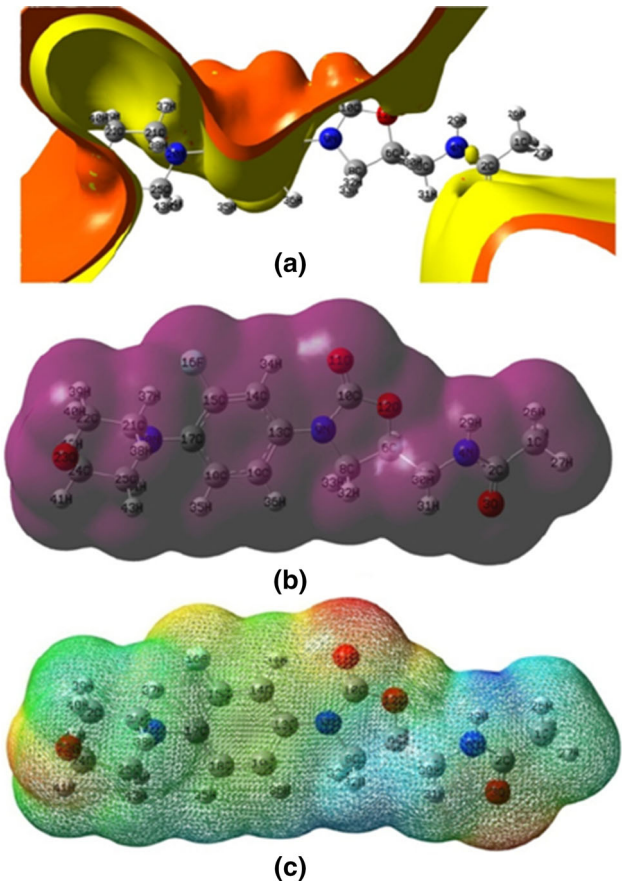

Fig. 4 (**a**) Electrostatic potential (ESP), (**b**) electron density (ED) and (**c**) the molecular electrostatic potential (MEP) map for Linezolid calculated at B3LYP/6-311G(d,p) level. (Color figure online)

The MEP map in molecule suggests that potential swings widely between oxygen atoms of nitro group (dark yellow) and proton of C–N–OH group (dark blue) in the five membered ring (blue). The oxygen atoms reflect the most electronegative region and have excess negative charge, and the hydrogen atoms attached to the C–N–OH group bear the brunt of positive charge (blue region). The different values of the electrostatic potential at the surface are represented by different colors. Potential increases in the order red < orange < yellow < green < blue. The color code of these maps is in the range between −0.1 a.u. (deepest red) to +0.1 (deepest blue) in all compounds, where blue indicates strongest attraction and red indicates the strongest repulsion.

5.2. Atomic net charges

The total atomic charges of Linezolid obtained by Mulliken [29] using B3LYP/6-31G(d,p) and B3LYP/6-311G(d,p) levels have been listed in Table 3. The charge distribution

Table 3 The charge distribution calculated by the Mulliken at B3LYP/6-31G(d,p)B3LYP/6-311++G(d,p) levels

Atoms	DFT/B3LYP	
	6-31G(d,p)	6-311G(d,p)
C1	−0.394883	−0.299552
C2	0.569710	0.317318
O3	−0.567585	−0.379215
N4	−0.520935	−0.416238
C5	−0.060099	−0.042535
C6	0.136561	−0.031239
H7	0.145720	0.146287
C8	−0.044081	−0.016451
N9	−0.609571	−0.532911
C10	0.798109	0.529226
O11	−0.542434	−0.345711
O12	−0.510606	−0.332578
C13	0.319052	0.230714
C14	−0.171307	−0.109706
C15	0.313388	0.250205
F16	−0.305080	−0.236051
C17	0.250382	0.106561
C18	−0.156158	−0.109473
C19	−0.153974	−0.129620
N20	−0.534696	−0.453549
C21	−0.062349	−0.095132
C22	0.045723	−0.000919
O23	−0.507470	−0.368353
C24	0.041087	0.005576
C25	−0.045612	−0.089993
H26	0.124354	0.102173
H27	0.150105	0.140342
H28	0.149696	0.139511
H29	0.291956	0.234877
H30	0.136648	0.124467
H31	0.153199	0.144599
H32	0.148619	0.131265
H33	0.159268	0.143624
H34	0.133659	0.150764
H35	0.116931	0.107671
H36	0.117100	0.101793
H37	0.128287	0.136422
H38	0.100670	0.099287
H39	0.098843	0.101068
H40	0.115356	0.112244
H41	0.115435	0.110537
H42	0.099147	0.098428
H43	0.103176	0.102731
H44	0.124658	0.121538

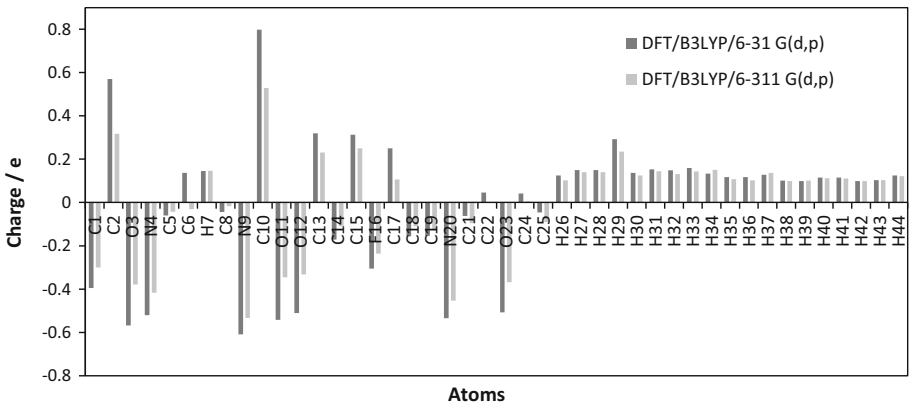

Fig. 5 Mulliken's plot of Linezolid

on the molecule has an important influence on the vibrational spectra. The corresponding Mulliken's plot is shown in Fig. 5 and it gives us information about the charge shifts relative to title molecule.

More charge density has been found at C10 than that of other ring carbon atoms. The high positive charge at C10 in Mulliken atomic charges are due to the effect of oxygen atom attached with C10. The nitrogen (N9) present in the five membered ring group has more negative charge than the nitro group nitrogen (N4, N20), which leads to the redistribution of electron density. The electron withdrawing character of the oxygen atom in the title molecule is demonstrated by a decrease of electron density on C5 and C6 atoms. In this study molecule, the Mulliken atomic charges show more negative values for the carbon atoms C21, C22 and C25 in B3LYP/6-311G(d,p) level. The above result shows that in B3LYP/6-311G(d,p) level the atomic charge changes are more sensitive to the changes in the molecular structure than B3LYP/6-31G(d,p) level.

6. UV–vis spectral studies and frontier molecular orbitals (FMOs)

In the UV–vis region with high extinction coefficients, all molecules allow strong π–π^* and σ–σ^* transition [33]. The experimental UV spectrum of Linezolid is plotted in Fig. 6. In an attempt to understand the nature of electronic transitions in terms of their energies and oscillator strengths, time-dependent DFT (TDDFT) calculations involving configuration interaction between the singly excited electronic states have been conducted. The calculated results involving the vertical excitation energies their molecular orbital contribution, oscillator strength (f) and wavelength are reported in Table 4. Due to the Frank–Condon principle, the maximum absorption peak (λ_{max}) in an UV–vis spectrum corresponds to vertical excitation. TD-DFT calculations predict three transitions in the near ultraviolet region for Linezolid molecule. The strong transitions at

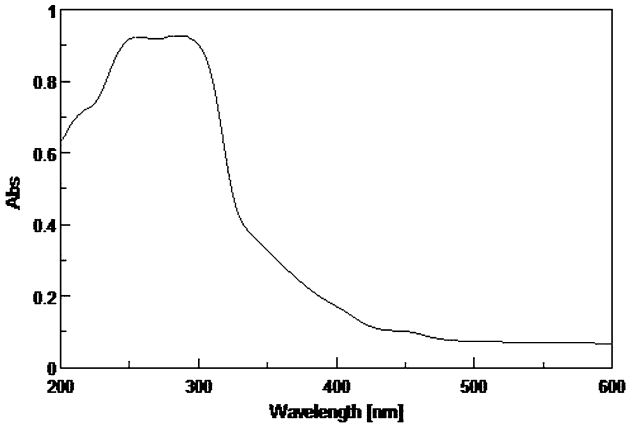

Fig. 6 Experimental UV spectrum of Linezolid

Table 4 TD-B3LYP singlet excitation energies and their molecular orbital contributions for Linezolid

State	TD-B3LYP/6-311G(d, p) level				
	Wavelength (nm)	Energy (eV)	Oscillator strength	Contribution	
Singlet-A″	279.99	4.8282	0.6312	H-2 → L + 1	0.16
				H → L	0.70
Singlet-A′	261.05	4.7495	0.5014	H-2 → L	0.12
				H → L + 1	0.61
Singlet-A″	222.81	5.5647	0.0013	H → L + 2	0.64
				H → L + 3	0.24
				H → L + 4	0.10

4.4282 eV (279.99 nm) with an oscillator strength f = 0.06312 and the other one 4.7495 eV (261.05 nm) with an oscillator strength f = 0.5014 have been observed. The maximum absorption wavelength corresponds to the electronic transition from the HOMO to (LUMO with 70 % contribution.

The electronic absorption corresponds to the transition from the ground to the first excited state and is mainly

Table 5 HOMO–LUMO energy values of Linezolid calculated at B3LYP method using 6-31G(d,p) and 6-311G(d,p) levels

Parameters	Method/levels	
	DFT/B3LYP/ 6-31G(d,p)	DFT/B3LYP/ 6-311G(d,p)
E_{HOMO} energy (eV)	−5.6120	−5.6439
E_{LUMO} energy (eV)	−0.6764	−0.5483
$\Delta E_{HOMO-LUMO}$ energy gap (eV)	4.9356	−5.0956
E_{HOMO-1} energy (eV)	−6.8556	−7.0164
E_{LUMO+1} energy (eV)	−0.6922	−0.4027
$\Delta E_{HOMO-1-LUMO+1}$ energy gap (eV)	−6.1634	−6.6137

described by one electron excitation from the HOMO to the LUMO. Commonly, the atom occupied by more densities of HOMO should have stronger ability for detaching electrons, whereas the atom with more occupation of LUMO should be easier to gain electrons. In order to evaluate the energetic behavior of the title molecule, the energies of HOMO, LUMO, LUMO +1, HOM −1 and their orbital energy gaps using B3LYP/6-31G(d,p) and 6-311G(d,p) basis sets are calculated and presented in Table 5. The pictorial illustrations of frontier molecular orbitals namely HOMO, HOMO −1, LUMO and LUMO +1, HOMO −2, HOMO −3, HOMO −4 for Linezolid are shown in Fig. 7. The HOMO lying at −5.09 eV is delocalized over π orbital and includes mixing of lone pairs of

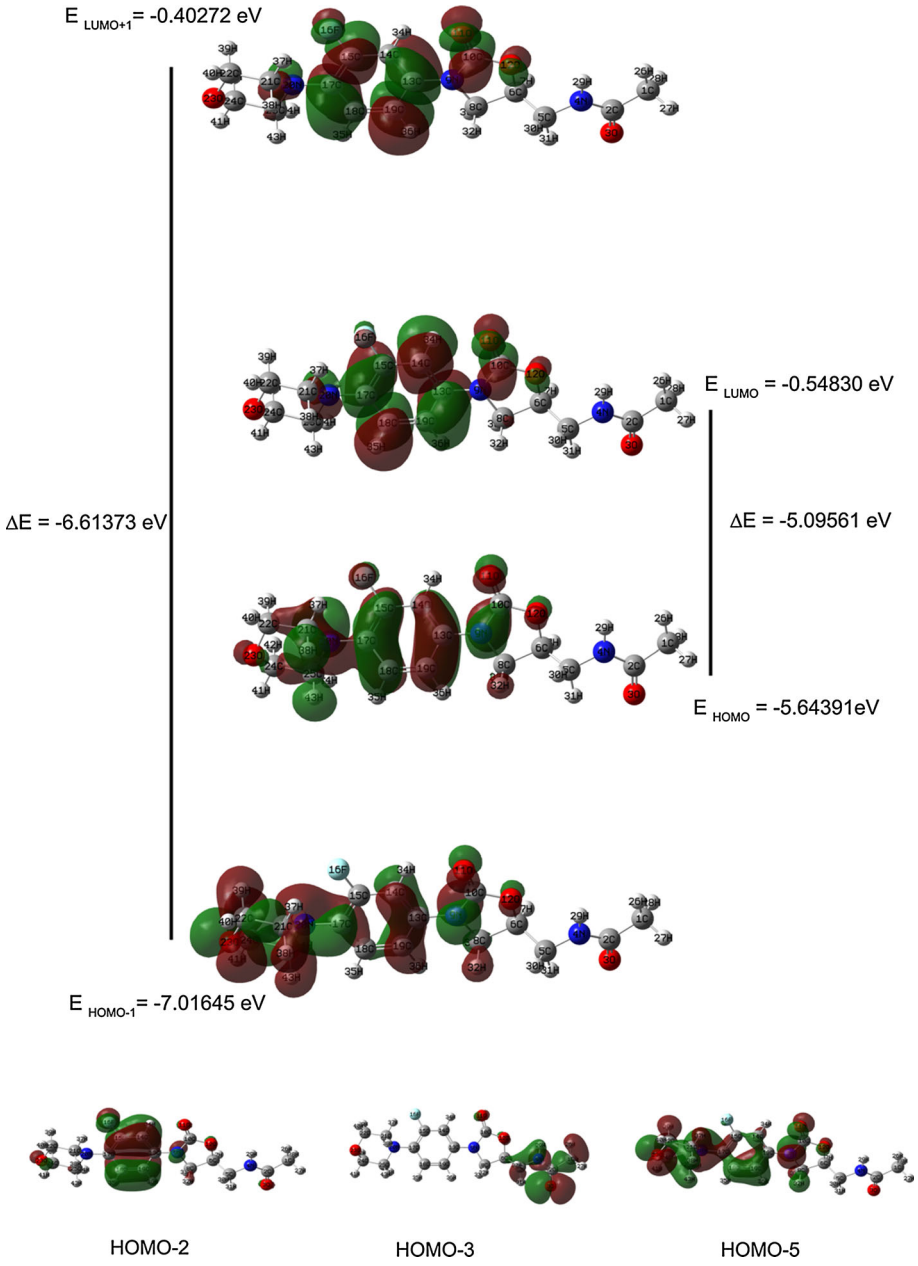

Fig. 7 The atomic orbital compositions of the frontier molecular orbital for Linezolid

electrons on all the oxygen as well as nitrogen atoms. The H-1, 1.37 eV below the HOMO is localized over the oxygen and nitrogen atoms on the rings. The H-2 is 1.45 eV below the homo is localized mainly on the carbon atoms of the six membered rings. The H-3 is 1.56 eV below the HOMO and has mainly of π bonding character along with some sigma bond character, whereas the LUMO lying at −0.5483 eV, is a π^* orbital, delocalized mainly on the carbon atoms of the six membered ring with some anti-bonding characters. From Table 5, it is evident that the absorption band centered around 220–260 nm arises mainly due to the four electronic transitions given by H → L + 1, H → L + 2, H → L + 3, H → L + 4 are assigned as π–π^* type, whereas the more intense band around 260–280 nm, having maximum oscillator strength (0.6312), corresponds to H → L transition and is mainly characterized as n–π^* type. The higher intensity of band corresponding to the n–π^* type transition is attributed to the presence of large number of free lone pairs of electrons available on four oxygen and three nitrogen atoms. It can be seen from the plots that the HOMO is spread more over the nitrogen and the carbon atoms in the six and five membered rings that shows appreciable amount of π bonding character. The LUMO is mainly found to be uniformly distributed over the carbon atoms in the six membered ring and reflects a lot of anti-bonding π character. The energy gap of HOMO–LUMO explains the eventual charge transfer interaction within the molecule and the frontier orbital energy gap in case of Linezolid is found to be −4.9356 and −5.0956 eV obtained at B3LYP/6-31G(d,p) and B3LYP/6-311G(d,p) levels, respectively.

7. Thermodynamic properties

Using the DFT/B3LYP with large (6-311G(d,p)) and small (6-31G(d,p)) basis set calculations, several thermodynamic properties like heat capacity, zero point energy, entropy of Linezolid have been calculated and are presented in Table 6. The difference in the values calculated by both the methods is only marginal. Scale factors have been recommended for an accurate prediction in determining the zero point vibration energy (ZPVE) and the entropy (S). The variation in the ZPVE seems to be insignificant. The total energies are found to decrease with the increase of the basis set dimension. Dipole moment reflects the molecular charge distribution and is given as a vector in three dimensions. Therefore, it can be used as descriptor to depict the charge movement across the molecule. Direction of the dipole moment vector in a molecule depends on the centers of positive and negative charges. The total dipole moment of Linezolid determined by B3LYP method using 6-31G(d,p) and 6-311G(d,p) levels are 3.6321 and 2.3520 Debye, respectively. All the thermodynamic data provide helpful information for the further study on the Linezolid. They can be used to compute the other thermodynamic energies according to relationships of thermodynamic functions and estimate directions of chemical reactions according to the second law of thermodynamics in thermo chemical field [33].

Table 6 The thermodynamic properties of Linezolid calculated at DFT/B3LYP/6-31G(d,p) and DFT/B3LYP/6-311G(d,p) levels

Parameters	DFT/B3LYP	
	6-31G(d,p)	6-311G(d,p)
SCF energy (a.u.)	−1,186.799	−1,187.065
Total energy (thermal) E_{total} (Kcal mol^{-1})	238.982	237.916
Vibrational energy, E_{vib} (Kcal mol^{-1})	237.204	236.139
Zero point vibrational energy (Kcal mol^{-1})	225.071	223.976
Specific heat, C_v (cal mol^{-1} K^{-1})	83.320	83.427
Entropy, S (cal mol^{-1} K^{-1})	164.971	165.654
Rotational constants (GHz)		
X	0.8748	0.8852
Y	0.0700	0.0700
Z	0.0688	0.0658
Dipole moment μ(Debye)		
μ_x	1.3253	0.8937
μ_y	−3.1542	−2.1011
μ_z	1.2194	0.5644
Total	3.6321	2.3520

8. Conclusions

The present investigation thoroughly analyzes the vibrational spectra, both infrared and Raman of Linezolid. The optimized geometries, harmonic vibrational wavenumbers and intensities of vibrational bands of Linezolid have been carried out using the DFT/B3LYP method using the standard 6-31G(d,p),6-311G(d,p) and M06-2X/6-31G(d,p) levels. The theoretical results have been compared with the experimental vibrations and it can be seen that the values obtained from M06-2X/6-31G(d,p) levels matches well with the experimental values. This DFT based quantum mechanical approach provides the most reliable theoretical information on the vibrational properties of Linezolid. The HOMO–LUMO analyses, MESP surface drawn and the electronic transitions identified for UV–Vis spectra may lead to understanding of properties and activity of Linezolid and the results are of assistance in the quest of the experimental and theoretical evidence for the title molecule in reaction intermediates and pharmaceuticals.

References

[1] S J Brickner *Curr. Pharm. Des.* **2** 175 (1996)
[2] Wroe David (2002-02-28). "An antibiotic to fight immune bugs". *The Age* Retrieved 2009-05-16.
[3] A P Wilson, J A Cepeda, S Hayman, T Whitehouse, M Singer and G Bellingan *J. Antimicrob. Chemother.* **58** 470 (2006)
[4] J P Abraham, I H Joe, V George, O F Nielson and V S Jayakumar *Spectrochim. Acta Part A* **59** 193 (2003)
[5] J Binoy, J P Abraham, I H Joe, V S Jayakumar, J Aubard and O F Nielson *J. Raman Spectrosc.* **36** 63 (2005)
[6] A D Becke *J. Chem. Phys*. **98** 5648 (1993)
[7] C Lee, W Yang and R G Parr *Phys. Rev. B* **37** 785 (1988)
[8] G Brancatelli, F Nicoló, S D Grazia, A M Monforte and A Chimirr *ActaCryst.* E **67** o1083 (2011)
[9] A K Jissy, S Konar and A Datta *Chem. Phys. Chem.* **14** 1219 (2013)
[10] A K Jissy and A Datta *J. Phys. Chem.* B **117** 8340 (2013)
[11] A K Jissy and A Datta *J. Phys. Chem. Lett.* **4** 1018 (2013)
[12] M J Frisch et al. *Gaussian 09* (Wallingford: Gaussian Inc.) (2009)
[13] P L Polavarapu *J. Phys. Chem.* **94** 8106 (1990)
[14] K Rajalakshmi, S Gunasekaran and S Kumaresan *Indian J. Phys*. **88** 733 (2014)
[15] T A Olszak, O M Peteres, N M Blaton and C J De Ranter *Acta Crystallogr. C* **51** 1304 (1995)
[16] V Krishnakumar and R J Xavier *Spectrochim. Acta Part A* **61** 253 (2005)
[17] D Sajan, H J Ravindra, N Misra and I H Joe *Vib. Spectrosc.* **54** 72 (2010)
[18] G Socrates *Infrared and Raman Characteristic Group Frequencies—Tables and Charts* 3rd edn. (Chichester: Wiley) (2001)
[19] S Sebastian and N Sundaraganesan *Spectrochim. Acta Part A* **75** 941 (2010)
[20] M M El-Nahass, M A Kamel, A F El-deeb, A A Atta and S Y Huthaily *Spectrochim. Acta Part A* **79** 443 (2011)
[21] N Sundaraganesan, C Meganathan and M Kurt *J. Mol. Struct*. **891** 284 (2008)
[22] V Arjunan, S Mohan, P Ravindran and C V Mythili *Spectrochim. Acta Part A* **72** 783 (2009)
[23] M S Weiss, M Brandi, J Suhnel, D Pal and R Hilgenfeld *Trends Biochem. Sci.* **26** 521 (2001)
[24] M Szafran, A Komasa and E B Adamska *J. Mol. Struct. Theochem.* **827** 101 (2007)
[25] S Gunasekaran, K Rajalakshmi, S Kumaresan *Spectrochim. Acta Part A* **112** 351 (2013)
[26] R M Silverstein, G C Bassler and T C Morrill *Spectrometric Identification of Organic Compounds* 4th edn. (New York: Wiley) p 245 (1981)
[27] V M Geskin, C Lambert and J L Bredas *J. Am. Chem. Soc*. **125** 15651 (2003)
[28] V Arjunan, I Saravanan, P Ravindran and S Mohan *Spectrochim. Acta Part A* **74** 642 (2009)
[29] V Krishnakumar, R Sangeetha, R Mathammal and D Barathi *Spectrochim. Acta Part A* **104** 77 (2013)
[30] S Gunasekaran, K. Rajalakshmi and S Kumaresan *Indian J. Phys.* **87** 723 (2013)
[31] M Arivazhagan, S Jeyavijayan and J Geethapriya *Spectrochim. Acta Part A* **104** 14 (2013)
[32] R S Mulliken *J. Chem. Phys*. **23** 1833 (1955)
[33[R Zhang, B Dub, G Sun and Y Sun *Spectrochim. Acta Part A* **75** 1115 (2010)